Identification of 4-(4-Aminopiperidin-1-yl)-7*H*-pyrrolo[2,3-*d*]pyrimidines as Selective Inhibitors of Protein Kinase B through Fragment Elaboration

John J. Caldwell,[†] Thomas G. Davies,[§] Alastair Donald,[†] Tatiana McHardy,[†] Martin G. Rowlands,[†] G. Wynne Aherne,[†] Lisa K. Hunter,[†] Kevin Taylor,[†] Ruth Ruddle,[†] Florence I. Raynaud,[†] Marcel Verdonk,[§] Paul Workman,[†] Michelle D. Garrett,[†] and Ian Collins*,[†]

Cancer Research UK Centre for Cancer Therapeutics, The Institute of Cancer Research, 15 Cotswold Road, Sutton, Surrey SM2 5NG, U.K., and Astex Therapeutics Ltd., 436 Cambridge Science Park, Milton Road, Cambridge CB4 0QA, U.K.

Received November 14, 2007

Fragment-based screening identified 7-azaindole as a protein kinase B inhibitor scaffold. Fragment elaboration using iterative crystallography of inhibitor−PKA−PKB chimera complexes efficiently guided improvements in the potency and selectivity of the compounds, resulting in the identification of nanomolar 6-(piperidin-1-yl)purine, 4-(piperidin-1-yl)-7-azaindole, and 4-(piperidin-1-yl)pyrrolo[2,3-*d*]pyrimidine inhibitors of PKBβ with antiproliferative activity and showing pathway inhibition in cells. A divergence in the binding mode was seen between 4-aminomethylpiperidine and 4-aminopiperidine containing molecules. Selectivity for PKB vs PKA was observed with 4-aminopiperidine derivatives, and the most PKB-selective inhibitor (30-fold) showed significantly different bound conformations between PKA and PKA−PKB chimera.

Introduction

Signaling through the PI3K−PKB−mTOR[a]cascade of intracellular kinases is a major component in the control of cell proliferation and survival.[1–4] It is clear that deregulation of this pathway is fundamentally associated with the development of several human cancers. For example, overexpression of the upstream tyrosine receptor kinase ERBB2 in breast and other tumors leads to constitutive signaling through protein kinase B.[5] Amplification or mutation of the gene encoding the PI3K 110α catalytic subunit, again leading to overactivation of the pathway, is frequently observed in human tumors, particularly ovarian and cervical carcinoma.[1,6] Deletion at the genetic level of the lipid phosphatase PTEN removes a negative regulator that normally functions to dephosphorylate the 3′-phosphatidylinositol substrates of PI3K and prevent PKB activation. Deletion of PTEN is frequently observed in human tumors, especially glioblastoma, endometrial, and prostate cancers.[1,4,7] PKB, particularly the β isoform, is itself commonly amplified at the genetic level, overexpressed, or overactivated.[1,8] Evidence of the therapeutic effect of inhibitors targeting this pathway has been reported. Analogues of the natural product rapamycin that inhibit mTOR function have shown antitumor efficacy in early clinical trials.[2] Dual inhibitors of PI3K/mTOR kinase function have shown antitumor activity in in vivo models.[9] An ATP-competitive inhibitor of PKB has also shown efficacy in animal models.[10] As a result of these observations, the PI3K−PKB−mTOR pathway is established as a promising locus of action for new molecularly targeted anticancer agents.[3,11–13]

There is significant interest in the discovery of new small molecule inhibitors of PKB, which may be ATP-competitive or may interact with regulatory domains in the protein.[11] Several classes of ATP-competitive inhibitors have been described, including pyridines,[10,14] azapanes,[15] indazole-4,7-diones,[16] toxoflavins,[17] isoquinoline-5-sulfonamides,[18,19] 6-phenylpurines,[20] and 4-phenylpyrazoles.[21] The application of structure-based design using crystallographic data from PKA[14b,f,g,18] or PKA−PKB chimeras[15,20,21] has been featured in the development of some of these chemical series. The high sequence homology between PKA and PKB in the ATP binding site (∼80%) supports the use of PKA or PKA−PKB chimeric proteins as surrogates of PKB. In this present work, a PKA−PKB chimera with three PKA → PKB mutations in the kinase active site of PKA was constructed (Val123 → Ala, Val104 → Thr, Leu173 → Met). An additional mutation, Gln181 → Lys, was incorporated outside the ATP-binding site to ameliorate the potential for Gln181 to disturb inhibitor binding in the presence of the Val123 → Ala substitution.[22] We have recently shown that a PKB-selective inhibitor[10] exhibits similar binding modes in both PKB and this PKA−PKB chimera, with a distinct binding conformation seen in PKA.[23] The major difference in binding mode was the repositioning of an inhibitor indole substituent within the ribose-binding pocket of the kinases, resulting from the Leu173 → Met switch between PKA and PKB. Although caution is required in translating crystallographic data observed with surrogates such as PKA or PKA−PKB chimeras to the interpretation of the structure–activity relationships of selective PKB ligands, the surrogates have nevertheless proved to be useful tools for the discovery of new inhibitor scaffolds. For convenience, a PKB−PKA chimera was therefore used for the iterative crystallographic studies described in this work. We have described the identification of 7-azaindole as a very low affinity, ATP-competitive ligand (PKBβ IC_{50} > 100 μM) in a crystallographic fragment screen.[20] The fragment was elaborated through structure-based design to the 6-phenylpurine **1** and subsequently to the potent PKB/PKA inhibitor **2** with activity in cells (Chart 1). The lead compound **2** and structurally related 4-phenylpyrazoles[21] were unselective for PKB inhibition over PKA. In this paper we describe the development of the 6-phenylpurine **1** into an alternative series of 4-piperidin-1-yl-7*H*-pyrrolo[2,3-*d*]pyrimidines with nanomolar potency and high ligand efficiency,[24] using iterative ligand−protein crystallography with the PKA−PKB chimera to guide improvements

* To whom correspondence should be addressed. Phone: +44 (0)208722-4317. Fax: +44 (0)2087224126. E-mail: Ian.Collins@icr.ac.uk.

[†] The Institute of Cancer Research.

[§] Astex Therapeutics Ltd.

[a] Abbreviations: PKB, protein kinase B (also known as Akt); PI3K, phosphatidylinositol-3 kinase; mTOR, mammalian target of rapamycin; PKA, protein kinase A.

10.1021/jm701437d CCC: $40.75
Published on Web 03/18/2008

Chart 1. Development of 6-Phenylpurine PKBβ Inhibitors[20]

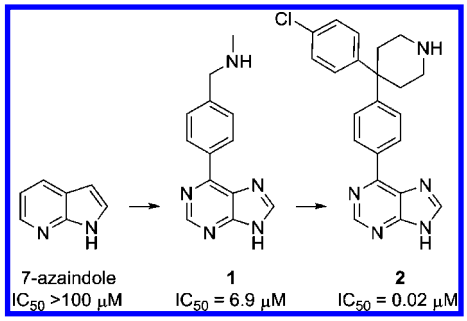

to inhibitor activity. Within this series, selective and unselective compounds with respect to PKB vs PKA were identified.

Results and Discussion

The addition of a benzylamine substituent onto the bicyclic hinge-binding fragment was an important step leading to **2**.[20] Our studies with 6-phenylpurines and isoquinoline-5-sulfonamide inhibitors of PKB[18] had shown that several productive binding positions were possible for the basic amine, reflecting the presence of two prominent acidic residues, Asp184 and Glu127 (PKA−PKB chimera numbering), in the ribose binding site of PKB.[25] We therefore sought to investigate alternatives to the 6-phenyl group as spacers between the purine bicycle and the amine in **1** and **2**. Changes to the heteroaromatic bicycle were also explored, focusing on replacing the heteroatoms to maintain the classical bidentate hydrogen-bonding to the hinge region of the kinase while modulating the lipophilicity and polar surface area of the compounds. Initial studies in the development of **2** had suggested that the balance of lipophilicity and hydrophilicity was a major determinant of cellular activity, presumably through control of penetration through the cell membrane.[20]

Replacement of the 6-phenyl spacer in **1** by piperidine was first targeted (Table 1). The importance of the basic amine was confirmed by the >10-fold drop in activity of the unsubstituted piperidine **3** and the 4-carboxamidopiperidine **4**. Gratifyingly, introduction of either a 4-aminomethyl or 4-amino substituent to the piperidine to give **5** or **6**, respectively, produced significantly more potent inhibitors of PKBβ than **1**. Both compounds showed very high ligand efficiency[24] (LE > 0.5 kcal mol^{-1} per non-H atom) indicating an excellent fit to the ATP-binding site. Although **5** and **6** were equipotent against PKBβ, a degree of selectivity (3- to 20-fold) versus PKA was observed, in contrast to the original hit **1** measured in the same assay protocols.

The binding modes of **1** (PDB code 2UVY), **5**, and **6** to the PKA−PKB chimera were compared (parts A, B, and C of Figure 1, respectively, and Figure 2). In all cases the bidentate hydrogen bonding of the purine to the hinge region of the kinase was maintained, with interactions seen between the N3 acceptor and N9 donor atoms of the inhibitor, and the backbone amides of Ala123 and Glu121, respectively. However, the position of the ligand's terminal amine was significantly different between **1**, **5**, and **6** because of the nonplanar structure of the piperidine spacer (Figure 2). In the structure of **1**−PKA−PKB the terminal methyl substituent of Met173 was packed directly under the benzene ring of **1**, forming favorable hydrophobic contacts. In contrast, for both **5** and **6** the chairlike conformation of the piperidine ring caused the ligands to intrude into this space, packing closely with the sulfur atom of Met173 and displacing the Cϵ methyl group by about 180° torsion about the Sδ−Cϵ bond.

As expected from other PKB inhibitor structures, the amine groups of **5** and **6** occupied a negatively charged region lined with acceptors. In the benzylamine **1** the secondary amine interacted directly with the Glu127 carboxylate and the backbone amide carbonyl of Glu170, while a water-mediated hydrogen bond was formed to the side chain of Asn171 (interatomic distances less than 3 Å). The side chain of Asp184 was oriented away from the inhibitor in this structure, forming a salt bridge with Lys72. In contrast, the amine of the aminomethylpiperidine **5** occupied the position of the water molecule seen in **1**−PKA−PKB. The side chain of Asp184 now adopted an alternative rotamer that brought the acid group into contact with the inhibitor. Direct hydrogen bonding to the backbone carbonyl of Glu170 was maintained, and a contact was made with the side chain of Asn171, but the hydrogen-bonding interaction with the acid of Glu127 was lost. When the terminal amine was attached directly to the piperidine in **6**, the amine interactions resembled that of **1**−PKA−PKB, with direct contacts to the Glu127 acid and the Glu170 carbonyl, and a water-mediated interaction to Asn171. As in **1**−PKA−PKB, the side chain of Asp184 was rotated away from the inhibitor in this structure. These divergent binding patterns in the ribose pocket were also observed for isoquinoline-5-sulfonamide inhibitors and reflect a broad region of energetically acceptable positions within this acceptor-rich subsite.[18]

The third point of the canonical PKB pharmacophore, an aromatic group capable of filling the lipophilic pocket in the P-loop near Phe54, was not present in **5** and **6**, and this region of protein exhibited varying amounts of disorder for these structures. In the structure of **1**−PKA−PKB the aromatic ring of Phe54 pointed toward the inhibitor binding site. Addition of an appropriate aromatic group to the inhibitor **1**, displacing Phe54, was an important step in the improvement of **1** to **2**,[20] and overlays of **5** and **6** with **2** suggested that potential vectors for further substitution with lipophilic groups analogous to the 4-chlorophenyl of **2** could originate either from the 4-position of the piperidine or from the carbon atom of the aminomethyl group of **5** (Figure 3A).

Despite submicromolar enzyme inhibitory potency for the hits, neither **5** nor **6** showed antiproliferative activity in cells. This was addressed through simple modifications of the purine heterocycle to decrease the hydrophilicity of the ligands (Table 1). Cellular potency was assayed by antiproliferative activity[26] in the PC3M human prostate cancer cell line, which is known to have an activated PI3K−PKB pathway and PTEN deletion.[27] A specific readout of target PKB inhibition in the cancer cells was also obtained by quantifying inhibition of phosphorylation of the downstream substrate GSK3β using a cell ELISA.[28] The bidentate hydrogen bonding potential of the heterocycle was maintained in all the compounds considered for synthesis. The 8-methylpurine **7** was less active than the parent purine **6**. Rearrangement of the purine to the allopurines **8** and **9**, with similar calculated[29,30] log *P* and topological polar surface area to **5** and **6**, was broadly tolerated in terms of PKBβ activity but did not result in significant cellular activity. However, replacement of one ring nitrogen from the five-membered ring by carbon to give the pyrrolo[2,3-*d*]pyrimidines **10** and **11** increased the calculated log *P*/TPSA ratio and led to observable antiproliferative activity and biomarker inhibition for both compounds. Substitution of a further nitrogen from the six-membered ring by carbon to give the azaindole **12** did not increase the cellular activity. The 4-aminopiperidine **10** was particularly promising, with reasonable PKBβ activity and some selectivity (8-fold) over PKA. A comparison of the structures of **6** and **10** complexed

Table 1. Development of 6-(Piperidin-1-yl)purines and Variation of the Bicyclic Heteroaromatic Group

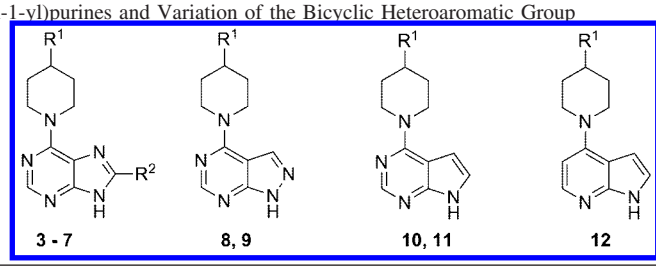

compd	R^1	R^2	PKBβ IC_{50} (nM)[a]	PKA IC_{50} (nM)[b]	SRB (PC3M) IC_{50} (μM)[c]	GSK3β ELISA (PC3M) IC_{50} (μM)[d]	TPSA (A^2)[e]	log P[f]
3	−H	−H	59000[g]	nd[h]	nd[h]	nd[h]	52	1.4
4	$-CONH_2$	−H	41000[g]	nd[h]	nd[h]	nd[h]	95	−0.13
5	$-CH_2NH_2$	−H	290 (±12)	890 (±9)	>50	nd[h]	78	0.17
6	$-NH_2$	−H	270 (±25)	4100 (±800)	>50	nd[h]	78	−0.33
7	$-NH_2$	−Me	110000[g]	nd[h]	nd[h]	nd[h]	78	0.34
8	$-NH_2$		830 (±12)	7300 (±627)	38	>30	78	0.05
9	$-CH_2NH_2$		920 (±80)	2400 (±340)	>50	>30	78	0.55
10	$-NH_2$		180 (±6)	1550 (±120)	48	15	66	0.44
11	$-CH_2NH_2$		770 (±19)	460 (±32)	32	11	66	0.94
12	$-NH_2$		880 (±107)	1933 (±97)	31	nd[h]	54	0.32

[a] Inhibition of PKBβ kinase activity in a radiometric filter binding assay. Mean (±SEM) for $n = 3$ determinations. Standard isoquinoline-5-sulfonamide inhibitor H-89[18] gave $IC_{50} = 0.59$ μM, SD ± 37% ($n = 20$) in this assay. [b] Inhibition of PKA kinase activity in a radiometric filter binding assay. Mean (±SEM) for $n = 3$ determinations. Standard isoquinoline-5-sulfonamide inhibitor H-8[18] gave $IC_{50} = 5.3$ μM, SD ± 38% ($n = 14$) in this assay. [c] Cell growth inhibition (sulforhodamine B colorimetric assay) determined in PC3M human prostate cancer cells. Mean of two independent determinations. Standard isoquinoline-5-sulfonamide inhibitor H-89[18] gave $IC_{50} = 18$ μM, SD ± 34% ($n = 20$) in this assay. [d] Single determination. Standard isoquinoline-5-sulfonamide inhibitor H-89[18] gave $IC_{50} = 15$ (±2) μM. [e] Calculated TPSA.[29] [f] Calculated log P.[29,30] [g] Mean of two independent determinations. [h] nd = not determined.

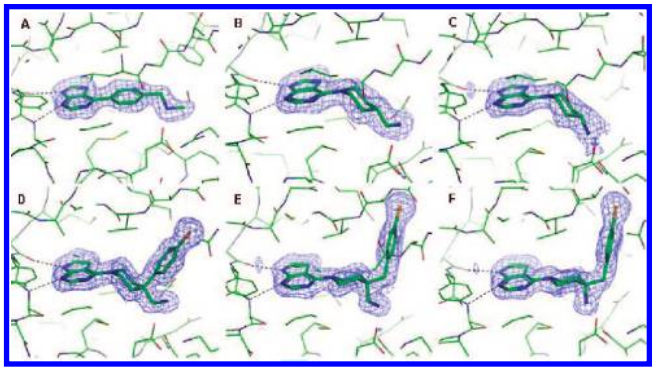

Figure 1. X-ray crystallographic structures of the ATP-binding site for complexes of **1**−PKA−PKB (A), **5**−PKA−PKB (B), **6**−PKA−PKB (C), **18**−PKA−PKB (D), **21**−PKA−PKB (E), and **25**−PKA−PKB (F). The final $2mF_o - DF_c$ electron density for inhibitors, contoured at 1σ, is shown in blue. Hydrogen bonds between the inhibitors and the hinge region of the kinase are denoted by dashed lines.

with the PKA−PKB chimera (data not shown) showed the ligand and protein conformations in the ATP-binding site to be identical. Although the selectivity for PKB over PKA in these compounds was low, the 4-aminopiperidine fragment was generally associated with more selectivity than the 4-aminomethylpiperidine moiety (compare **6** vs **5**, **8** vs **9**, and **10** vs **11**).

To improve the PKBβ inhibitory activity of the series, the addition of a lipophilic group to make contact with the P-loop was targeted. Initially the unselective 4-aminomethylpiperidine scaffold **11** was investigated by analogy with the development of 6-phenylpurine and 4-phenylpyrazole inhibitors.[20,21] Appending a phenyl ring to the aminomethyl group in **13** gave a moderate increase in activity (Table 2). A much more significant 10-fold increase was seen when 4-chloro substitution was introduced to the aromatic ring in **14**, recapitulating structure–activity relationships observed in the evolution of **2**[20] and isoquinoline-5-sulfonamide PKB inhibitors.[18] Although unselective versus PKA, the more potent compound **14** showed improved cellular activity in the PC3M cell line and also in U87MG glioblastoma cells compared to **11** and **13**, consistent with antiproliferative activity occurring through target modulation. The U87MG human tumor cell line has been shown to have elevated signaling through the PI3K−PKB−mTOR pathway and is especially relevant for the assessment of molecular therapeutics targeted to the pathway.[9] The improvement in cellular activity was attributed to both the increased enzyme inhibition and the increased lipophilicity of **14** (calculated log $P = 3.2$; TPSA = 66 $Å^2$). Switching back to the more polar purine hinge-binding motif **15** also caused a small (2.5-fold) drop in inhibitory potency, which together with reduced cell penetration may be reflected in the reduced antiproliferative effect in PC3M cells. Conversely, changing the pyrrolo[2,3-*d*]pyrimidine to the 7-azaindole **16** maintained the enzyme inhibitory activity and was accompanied by an increase in the cellular inhibition of PKB as measured by cell ELISA. Compounds **13**−**16** were prepared and tested as racemic mixtures. At this stage alternative, achiral scaffolds were targeted by applying the structure–activity relationships and crystallographic binding modes from the foregoing studies to the elaboration of geminal-substituted 4-piperidines. In general, the pyrrolo[2,3-*d*]pyrimidine hinge-binding motif was preferred over 7-azaindole because it offered a useful combination of enzyme potency, cellular activity, and synthetic accessibility.

Moving the aryl group of **14** to the 4-position of the 4-aminomethylpiperidine gave the geminally substituted compound **18** and its purine and 7-azaindole congeners **17** and **19**, respectively. Good PKBβ inhibitory activity was seen in vitro with no selectivity over PKA. The antiproliferative and cellular target inhibition activities of the pyrrolo[2,3-*d*]pyrimidine **18** were at or below 1 μM for the first time in this series. However, determination of general kinase selectivity indicated that some of this improvement in antiproliferative activity might reflect off-target effects (see below). Homologation of the lipophilic substituent to generate the 4-(4-chlorophenylmethyl)-4-aminomethylpiperidines **20** and **21** gave potent PKBβ inhibitors, again with no selectivity over PKA but with decreased cellular

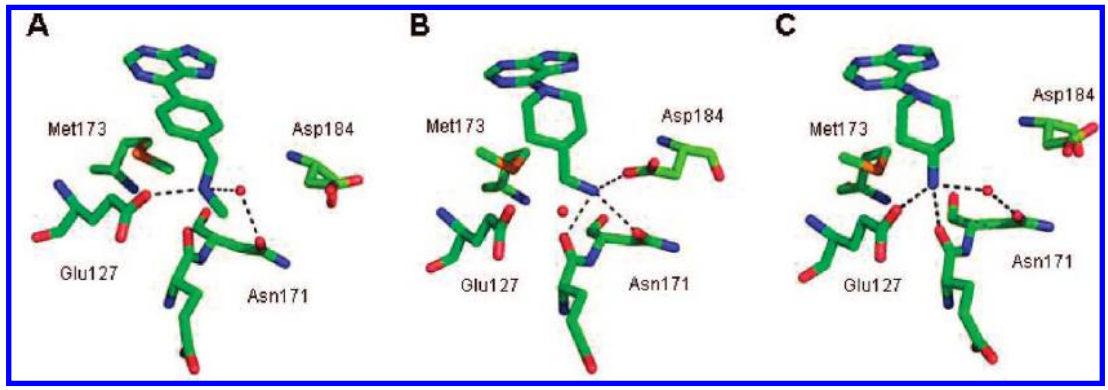

Figure 2. Detail of the X-ray crystallographic structures for the complexes of **1**−PKA−PKB (A), **5**−PKA−PKB (B), and **6**−PKA−PKB (C) showing the ribose-binding pocket. The inhibitors and key residues are represented as solid sticks coloured by atom type (carbon = green). Key water molecules are represented as red spheres, and polar contacts discussed in the text are indicated by dashed lines.

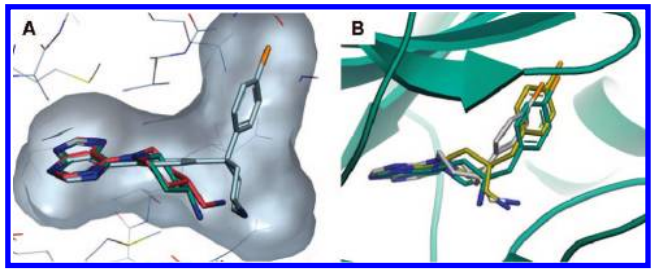

Figure 3. (A) Overlay of **2**−PKA−PKB (gray), **5**-PKA−PKB (red), and **6**-PKA−PKB (green) in the ATP-binding site. The ATP site of **2**−PKA−PKB is depicted as a gray surface. (B) Overlay of **18**−PKA−PKB (gray), **21**−PKA−PKB (gold), and **25**−PKA−PKB (green) in the ATP-binding site. The protein structure for **25**−PKA−PKB is shown as a cartoon representation.

activity (e.g., compare **21** vs **18**). The alternative geminal substituted 4-aminopiperidines showed a different profile. With the aryl group directly attached to the 4-position, compounds **22** and **23** were potent PKBβ inhibitors with no selectivity over PKA. However, homologation of the 4-chlorophenyl substituent to the 4-(4-chlorophenylmethyl) group in **24** and **25** introduced selectivity (11- to 30-fold) for PKBβ over PKA. The contrast between the very poor cellular activities of the purines and the better activities of the pyrrolo[2,3-*d*]pyrimidines in compounds **22–25** was more marked than had been seen in the 4-aminomethylpiperidine compound set **17–21**. Comparison of the enzyme inhibition and cellular effects of the potent, unselective inhibitor **18** and the most selective inhibitor **25** implied that the high antiproliferative activity of **18** could be due to off-target inhibitory effects. The kinase inhibitory profiles of **18** and **25** in a panel of 21 enzymes were investigated.[31] Compound **18** showed activity (>60% inhibition at 1 μM) toward 10 kinases, including receptor and cytoplasmic tyrosine kinases (e.g., FLT3, SRC) and non-AGC serine/threonine kinases (e.g., CHK1, CHK2) as well as other AGC kinases (e.g., PKC, ROCK2, RSK2, p70S6K). In contrast compound **25** was much less promiscuous with activity seen only against two other enzymes, both in the AGC family (p70S6K, ROCK2). The inhibition of p70S6K by **25** as measured in a radiometric filter binding assay was IC_{50} = 120 nM, indicating a 20-fold selectivity for inhibition of PKBβ over p70S6K.

The structures of **18**, **21**, and **25** bound to the PKA−PKB chimera were determined (parts D, E, and F of Figure 1, respectively). The binding modes were found to be consistent with the earlier derivatives with the heteroaromatic bicycle serving to anchor the molecules in the ATP-binding site via hydrogen-bonding interactions with the hinge. Variations in the exact orientation and conformation of the piperidine and terminal amine were seen between the compounds. The conformationally flexible piperidine spacer adapted to optimally position the amine and lipophilic group as the connectivities between these functionalities were varied (Figure 3B). The 4-aminomethylpiperidine **18** adopted a similar conformation to the unsubstituted precursor **5**, with near-planar geometry at the piperidine nitrogen. In contrast, both the 4-aminomethylpiperidine **21** and the 4-aminopiperidine **25** showed a more planar orientation of the piperidine ring relative to the plane of the aromatic heterocycle, with a more pronounced pyramidal geometry at the piperidine nitrogen. This change in geometry is presumably required so that the more extended 4-chlorobenzyl substituent can still occupy the P-loop binding pocket. The possibility of varying degrees of conjugation between the piperidine nitrogen lone pair and the heteroaromatic substituent, and the subsequent variation in geometry of the piperidine nitrogen in these inhibitors, allows the saturated ring to respond to varying substitution patterns with a range of energetically accessible bound conformations. The same divergent pattern in amine binding was seen for the piperidine scaffolds in these elaborated compounds as was seen with **5** and **6**. Thus, the 4-aminomethylpiperidines **18** and **21** interacted with Asp184, Asn171, and Glu170, whereas for the 4-aminopiperidine **25** the major interactions were to Glu127 and Glu170, with Asp184 adopting the rotamer for interaction with Lys72. The lipophilic 4-chlorophenyl and 4-chlorobenzyl substituents were directed into a hydrophobic pocket defined principally by the side chains of Thr51, Gly52, Phe54, Val57, Lys72, Leu74 and the backbone carbonyls of Thr51 and Gly55. However, the 4-chlorobenzyl substituents of **21** and **25** projected more deeply into this pocket than the 4-chlorophenyl group of **18**.

We have previously shown how the 40-fold selectivity for PKB over PKA found for an indazole pyridine PKB ligand[10] could be rationalized by comparing the interactions formed by the inhibitor bound with PKA, PKB, and PKA−PKB chimera.[23] In that case, the PKA−PKB chimera was found to bind the ligand in a pose more closely resembling that of PKB than PKA. For the selective PKB inhibitor **25**, we were unable to obtain sufficiently high-resolution data for the inhibitor−PKB complex. Nevertheless, the structures of **25** bound to PKA and the PKA−PKB chimera were compared to help understand the origin of its selectivity. Although the pyrrolo[2,3-*d*]pyrimidines overlaid well, a marked difference in the conformations of the piperidine rings and consequently in the position of the 4-chlorobenzyl groups was seen such that the aryl groups were at approximately 90° to one another in the two complexes.

Table 2. Addition of the Lipophilic Group to the 4-Aminomethyl- and 4-Aminopiperidines

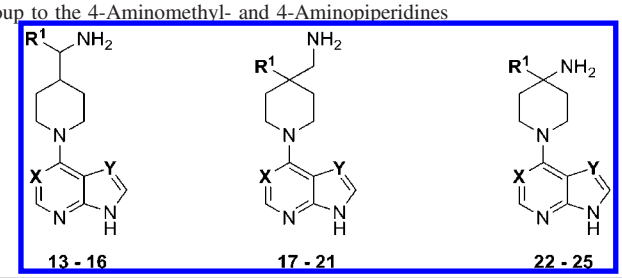

compd	X	Y	R^1	PKBβ IC_{50} (nM)[a]	PKA IC_{50} (nM)[b]	SRB PC3M IC_{50} (μM)[c]	GSK3β ELISA PC3M IC_{50} (μM)[d]	SRB U87MG IC_{50} (μM)[e]	GSK3β ELISA U87MG IC_{50} (μM)[f]
13	N	CH	Ph−	246 (±33)	726 (±67)	38	>30	nd[g]	nd[g]
14	N	CH	4-Cl-Ph−	25 (±4)	54 (±11)	7.4	7.5	6.0	2.0
15	N	N	4-Cl-Ph−	71 (±17)	27 (±4)	23	nd[g]	nd[g]	nd[g]
16	CH	CH	4-Cl-Ph−	12 (±2)	3 (±0.5)	5.3	2.0	3.5	<1
17	N	N	4-Cl-Ph-	16 (±9)	3 (±0.5)	5.7	1.3	nd[g]	nd[g]
18	N	CH	4-Cl-Ph−	8 (±3)	5 (±0.8)	1.0	0.5	0.52	0.59
19	CH	CH	4-Cl-Ph−	25 (±2)	3 (±0.7)	16	1.4	nd[g]	nd[g]
20	N	N	4-Cl-(C_6H_4)CH_2−	3 (±0.9)	7 (±1.5)	20	1.7	nd[g]	nd[g]
21	N	CH	4-Cl-(C_6H_4)CH_2−	5 (±2)	9 (±2)	15	1.4	4.3	0.45
22	N	N	4-Cl-Ph−	7 (±1.4)	23 (±4)	>50	nd[g]	nd[g]	nd[g]
23	N	CH	4-Cl-Ph−	7 (±0.9)	15 (±2)	8	0.6	4.7	<1
24	N	N	4-Cl-(C_6H_4)CH_2−	25 (±3)	286 (±42)	>50	nd[g]	nd[g]	nd[g]
25	N	CH	4-Cl-(C_6H_4)CH_2−	6 (±1.5)	168 (±36)	12	3.0	5.0	0.66

[a] Inhibition of PKBβ kinase activity in a radiometric filter binding assay. Mean (±SEM) for $n = 3$ determinations. Standard isoquinoline-5-sulfonamide inhibitor H-89[18] gave $IC_{50} = 0.59$ μM, SD ± 37% ($n = 20$) in this assay. [b] Inhibition of PKA kinase activity in a radiometric filter binding assay. Mean (±SEM) for $n = 3$ determinations. Standard isoquinoline-5-sulfonamide inhibitor H-8[18] gave $IC_{50} = 5.3$ μM, SD ± 38% ($n = 14$) in this assay. [c] Cell growth inhibition (sulforhodamine B colorimetric assay) determined in PC3M human prostate cancer cells. Mean of two independent determinations. Standard isoquinoline-5-sulfonamide inhibitor H-89[18] gave $IC_{50} = 18$ μM, SD ± 34% ($n = 20$) in this assay. [d] Single determination. Standard isoquinoline-5-sulfonamide inhibitor H-89[18] gave $IC_{50} = 15$ (±2) μM. [e] Cell growth inhibition (sulforhodamine B colorimetric assay) determined in U87MG human glioblastoma cancer cells. Mean of two independent determinations. Standard isoquinoline-5-sulfonamide inhibitor H-89[18] gave $IC_{50} = 15$ μM, SD ± 15% ($n = 19$) in this assay. [f] Single determination. Standard LY294002 gave $IC_{50} = 8.1$ (±3.0) μM. [g] nd = not determined.

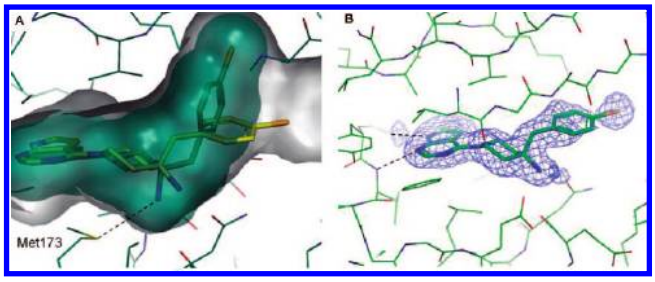

Figure 4. (A) Overlay of **25**−PKA−PKB (green) and **25**−PKA (gold) in the ATP site. The surface of PKA−PKB is shown in gray, the surface of **25** when bound to PKB is shown in green, and the putative $S\cdots N^+$ interaction is denoted by a dashed line. (B) Structure of **25**−PKA in the region of the ATP site. The final $2mF_o - DF_c$ electron density for the inhibitor, contoured at 1σ, is shown in blue. Hydrogen bonds to the hinge region of the kinase are denoted by dashed lines.

Importantly in PKA−PKB (and presumably PKB), but not in PKA, **25** exhibited productive binding of the chlorobenzyl with the lipophilic pocket at the P-loop (Figure 4A), potentially providing an explanation for the observed selectivity. The differences in binding between PKA and PKA−PKB appear to arise because of the Leu173 → Met change at the base of the ATP cleft. The ability of the 4-chlorobenzyl substituent to access the P-loop pocket is dependent on a specific conformation of the piperidine ring in which the charged amine forms a close contact with the sulfur of the Met173 side chain ($r_{S\cdots N} = 3.6$ Å), in addition to interactions with acceptors in the basic pocket. An analysis of the Cambridge Structural Database (see Supporting Information) suggested that such $S\cdots NH_3^+$ interactions are favorable to binding, and in PKA−PKB the presence of methionine at this point therefore provides an energetically suitable environment for the binding of this basic group. In contrast, the substitution by leucine at this position in PKA does not provide a favorable environment in which to locate the amine functionality because of its inability to compensate for the associated dehydration penalty. To accommodate the inhibitor in this case, the piperidine adopts an alternative conformation in which the amino group is displaced by >1 Å from its position in PKA−PKB while still maintaining its interaction with residues lining the basic pocket. However, this conformation no longer provides a suitable vector by which the 4-chlorobenzyl substituent can form the favorable P-loop interactions required for high affinity binding. In contrast to its binding to PKA−PKB, the aryl group is partially disordered, as judged by relatively weak electron density and high *B*-factors, with the dominant conformation projecting parallel to the P-loop into a solvent exposed site (Figure 4B). Consistent with the lack of interactions formed with this region of PKA, the tip of the P-loop also exhibits disorder, with broken electron density indicating a range of possible conformations.

The structure–activity and X-ray crystallographic data presented here suggest that the basic amine and lipophilic binding elements in this chemical series may influence the selectivity of the inhibitors for PKB vs PKA. The flexible conformations afforded by the piperidine linker and the variable hybridization of the piperidine nitrogen appear to be key to exploiting the relatively subtle differences between PKA and PKB in this part of the kinase domain. Selectivity for inhibition of PKB over PKA may be desirable because PKA activity has been described as both oncogenic and tumor-suppressing, depending on cellular context.[32,33] Selective ATP-competitive inhibitors of PKB vs PKA have been recently reported.[10,14f,g] High specificity for PKB over PKA has also been achieved with ligands interacting with the PH domain of PKB.[34,35]

The effect of the selective inhibitor **25** on the PI3K−PKB−mTOR−S6 pathway was assessed in U87MG and PC3M cell lines (Figure 5). Two divergent arms of the signaling network downstream of PKB were blocked, with reductions seen in the

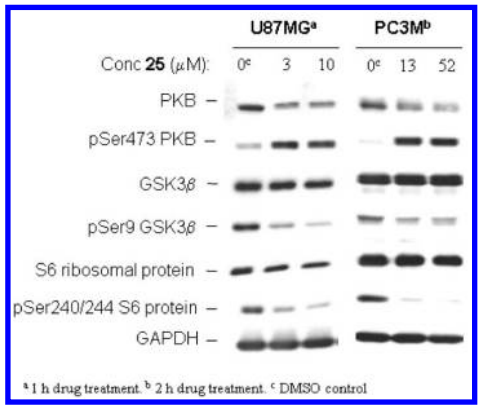

Figure 5. Western blot showing the effect of compound **25** on the phosphorylation state of components of the PI3K−PKB−mTOR pathway in U87MG glioblastoma and PC3M prostate human cancer cells. GAPDH was used as the loading control.

levels of pGSK3β and pS6 ribosomal protein as expected for a PKB inhibitor. An increase in the levels of pSer473-PKB was also seen, indicative of increased levels of signaling to PKB as a compensatory response to blockade of the pathway. This is consistent with a proposed feedback inhibition pathway from activated p70S6K downstream of PKB to the upstream regulator IRS1,[36] or an alternative mTORC1-independent route,[37] and has been observed with other inhibitors of PKB.[20] Importantly, this compensatory activation of signaling to PKB is overcome by the inhibitors such that an overall reduction in signaling throughput downstream of PKB is still achieved. Targeted inhibition of the pathway as shown by the Western blots and cell ELISA assays was seen at concentrations (IC_{50} = 0.66–3.1 μM) consistent with the biochemical inhibitory activity of **25**. Given that the $K_{m,ATP}$ for PKBβ has been determined as 30 μM [17] and assuming an approximate intracellular ATP concentration of 10 mM and also that $K_i \approx 0.5\ IC_{50}$ for the ATP-competitive inhibitor **25** in the biochemical assay,[38] then a 1 μM concentration of **25** would be expected to produce approximately 50% inhibition of intracellular PKB ($v/V_{max} = [S]/([S] + K_m(1 + [I]/K_i))$). The inhibition of cell growth by **25** and other compounds in this series generally required higher concentrations than this. Whereas the cellular ELISA and other pharmacodynamic assays demonstrate that the compounds do inhibit the target pathway, the sensitivity of tumor cells to that blockade is a function of cellular dependence on the pathway, which may vary considerably between cell types.[12,39] It is possible that profound inhibition of signaling through the pathway is required to provoke an antiproliferative or apoptotic effect. Taking into account potential differences in compound permeability and selectivity, the structure–activity relationships in this series of inhibitors with respect to biochemical inhibition of PKBβ generally track with the cellular biomarker effects and antiproliferation.

Measurement of the in vitro metabolism of **25** was made by tandem liquid chromatography–mass spectrometry (LC−MS) following incubation in mouse and human liver microsomes.[40] Compound **25** was moderately metabolized in mouse liver microsomes competent for phase I and phase II metabolism, with 87% of the parent compound remaining after 30 min of incubation at a concentration of 10 μM. In human liver microsomes 79% of **25** remained after 30 min of incubation at a concentration of 10 μM in the presence of cofactors suitable for phase I metabolism. Identification of metabolites in these incubations revealed an oxidation product (M + 16). The potential for inhibition of cytochrome P450 isoforms by **25** was measured in human liver microsomes.[41] Compound **25** showed IC_{50} > 50 μM vs CYP1A2, CYP2A6, CYP2C19, CYP3A4, and CYP2E1. Very low inhibition (IC_{50} = 10–50 μM) was seen for CYP2C9, while significant inhibition was seen with CYP2D6 (IC_{50} = 1–10 μM). The pharmacokinetic (PK) profile of **25** was determined following iv and oral dosing at 25 mg kg^{-1} to female BALB/c mice in 10% DMSO 0.1% Tween-20 in saline (Table 3). Compound **25** was widely distributed (V_{ss} = 0.25 L) but cleared very quickly from the general circulation with a plasma clearance higher than that of mouse liver blood flow. The compound was short-lived with a plasma half-life of less than an hour. However, the high volume of distribution was confirmed by significant tissue distribution with spleen to plasma concentration ratio of 7:1. Following oral administration of the same dose of compound **25**, plasma concentrations reached levels of 432 nM. The overall bioavailability was low but measurable (F_{oral} = 8.5%). Although clearly requiring optimization in terms of increasing the half-life and oral bioavailability, the PK performance of the 4-(piperidin-1-yl)pyrrolo[2,3-*d*]pyrimidine scaffold **25** was encouraging with good distribution to tissue seen.

Table 3. Pharmacokinetic Parameters of **25** in Mice

plasma PK parameters	**25** iv (25 mg kg^{-1})	**25** po (25 mg kg^{-1})
$T_{1/2}$ (h)	0.95	0.57
T_{max} (h)	0.083	0.5
C_{max} (nmol L^{-1})	6357	432
AUC (h nmol L^{-1})	4619	392
V_{ss} (L)	0.25	
Cl_p (L h^{-1})	0.325	

Conclusions

Novel potent 4-(4-substituted-piperidin-1-yl)-7*H*-pyrrolo[2,3-*d*]pyrimidine ATP-competitive inhibitors of PKB were discovered starting from the 6-phenylpurine **1**, itself derived from the identification of 7-azaindole as a weakly binding fragment in a high-throughput crystallography screen. X-ray crystallography of inhibitor−PKA−PKB chimera complexes was coupled with the measurement of compound activity in enzyme assays and relevant cellular mechanistic assays to efficiently guide improvements in the potency and selectivity of the compounds, resulting in the identification of nanomolar inhibitors of PKBβ. The cellular activity of the purine inhibitors was improved through modulation of the lipophilicity of the purine heterocycle by replacement with less polar 7*H*-pyrrolo[2,3-*d*]pyrimidine and 7-azaindole. A divergence in the binding mode of the basic amine was seen between 4-aminomethylpiperidine and 4-aminopiperidine containing molecules. Selectivity for PKB vs PKA was observed with 4-aminopiperidine derivatives, and the most PKB-selective (30-fold) inhibitor **25** showed a significantly different binding mode between PKA and PKA−PKB chimera. Compound **25** showed inhibition of relevant molecular biomarkers on the PI3K−PKB−mTOR pathway in cells. With excellent ligand efficiency (LE = 0.47 kcal mol^{-1} per non-H atom), **25** is a potential lead and a useful tool for investigation of inhibition of the PKB pathway.

Experimental Section

Synthetic Chemistry. Simple 6-(piperidin-1-yl)purine analogues **3**−**6** of the hit compound **2** were prepared by direct nucleophilic substitution of 6-chloropurine **26** (Scheme 1). Alternative bicyclic hinge-binding groups were incorporated into compounds **7**–**12** by similar reactions (Scheme 2). The use of ethanol rather than *n*-butanol as solvent and lower temperatures gave higher yields for the displacement of 4-chloro-1*H*-pyrazolo[3,4-*d*]pyrimidine[42] **30**

Scheme 1[a]

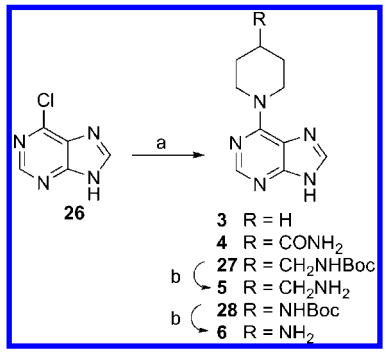

[a] Reagents and conditions: (a) 4-substituted piperidine, Et_3N, *n*-BuOH, 100 °C; (b) 2 M HCl, room temp.

Scheme 2[a]

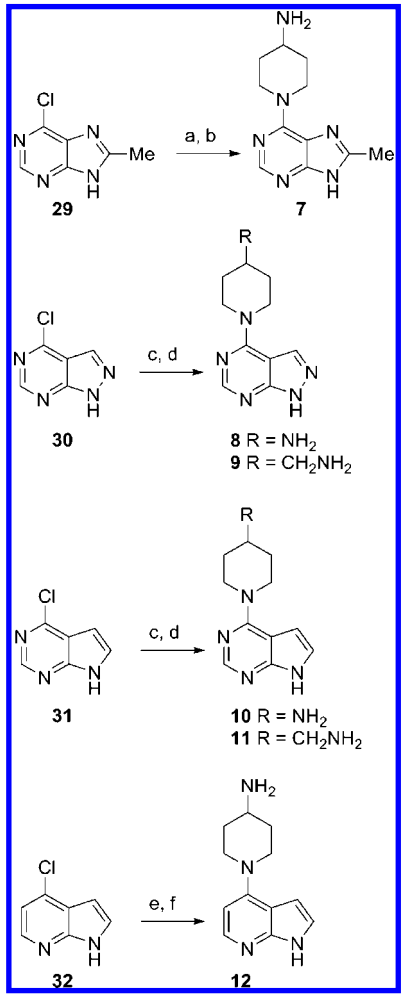

[a] Reagents and conditions: (a) 4-(Boc-amino)piperidine, Et_3N, *n*-BuOH, 100°C; (b) 2 M HCl_{aq}, room temp; (c) 4-(Boc-amino)piperidine or 4-*N*-(Boc-aminomethyl)piperidine, Et_3N, EtOH, 80°C; (d) 4 M HCl−dioxane, room temp; (e) 4-(Boc-amino)piperidine, NMP, microwave, 160°C; (f) CF_3CO_2H, CH_2Cl_2, 0°C.

by amines. The less reactive 4-chloro-1*H*-pyrrolo[2,3-*b*]pyridine[43] **32** required microwave heating for successful reaction.[44] Elaboration of the 4-(aminomethyl)piperidine scaffold to the aryl substituted compounds **13–16** was achieved by prior construction of the substituted piperidine through reductive amination of commercially available 4-ketopiperidines before coupling to the heteroaromatic bicycle (Scheme 3).

The geminal substituted piperidines **17–25** were prepared by two related divergent routes (Scheme 4). Double alkylation of (4-

Scheme 3[a]

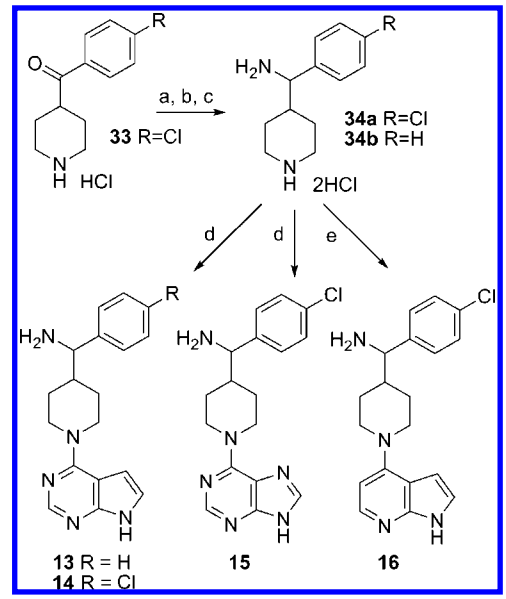

[a] Reagents and conditions: (a) $(Boc)_2O$, Et_3N, MeCN, room temp; (b) NH_4OAc, $NaCNBH_3$, MeOH, reflux; (c) 2 M HCl_{aq}, MeOH, room temp; (d) **26** or **31**, Et_3N, *n*-BuOH, 100°C; (e) **32**, NMP, microwave, 155°C.

Scheme 4[a]

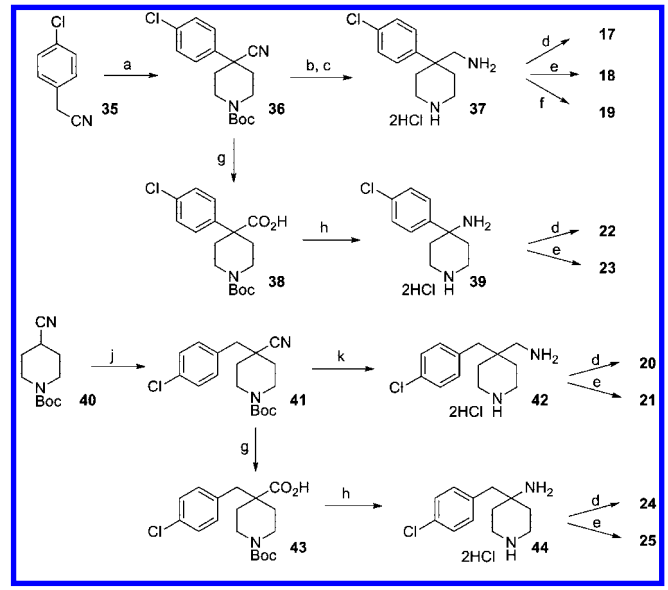

[a] Reagents and conditions: (a) NaH, $(ClCH_2CH_2)_2NBoc$, DMF, 60°C; (b) Raney Ni, H_2 (1 atm), EtOH, room temp; (c) 2 M HCl_{aq}, MeOH, room temp; (d) **26**, Et_3N, *n*-BuOH, 100°C; (e) **31**, Et_3N, *n*-BuOH, 100°C; (f) **32**, Et_3N, NMP, microwave, 155°C; (g) (i) 6 M HCl_{aq}, reflux; (ii) NaOH, $(Boc)_2O$, room temp; (h) (i) *i*-BuOCOCl, Et_3N, THF, room temp; (ii) NaN_3, H_2O−THF, room temp; (iii) toluene, 90°C; (j) LDA, $(4\text{-}ClC_6H_4)CH_2Cl$, THF, −78 °C; (k) (i) 4 M HCl−dioxane, MeOH, room temp; (ii) 1 M BH_3−THF, THF, room temp.

chlorophenyl)acetonitrile **35** with the nitrogen mustard bis-(2-chloroethyl)carbamic acid *tert*-butyl ester[45] gave the common intermediate nitrile **36**.[46] Reduction of the nitrile **36** with Raney nickel produced the 4-chlorophenyl-4-aminomethylpiperidine fragment **37** from which compounds **17–19** were prepared using the displacement reactions described before. Alternatively, the intermediate nitrile **36** was hydrolyzed to the carboxylic acid **38**. The acidic hydrolysis removed the carbamate protecting group that was reinstalled in a separate step. A Curtius rearrangement sequence via the acyl azide[47] was used to transform the acid **38** into the 4-chlorophenyl-4-aminopiperidine **39**, which was coupled to 6-chloro-

purine **26** and 4-chloro-7*H*-pyrrolo[2,3-*d*]pyrimidine[48] **31** to give compounds **22** and **23**, respectively.

To prepare the piperidines substituted at the 4-position with benzylic groups, 4-cyanopiperidine-1-carboxylic acid *tert*-butyl ester **40** was alkylated[49] with 4-chlorobenzyl chloride to give the intermediate nitrile **41**. N-Deprotection of **41** followed by reduction of the nitrile with borane−THF gave 4-(4-chlorophenyl)-4-aminomethylpiperidine **42**, which was coupled to the heteroaromatic chlorides as before to give compounds **20** and **21**. The acid hydrolysis and Curtius rearrangement sequence was applied to intermediate **41** to yield the 4-(4-chlorobenzyl)-4-aminopiperidine **44**. The piperidine **44** was coupled to 6-chloropurine **26** and 4-chloro-7*H*-pyrrolo[2,3-*d*]pyrimidine **31** to provide inhibitors **24** and **25**, respectively. We have recently described a more efficient and direct one-pot route to 4-benzyl-4-aminopiperidines such as **44**, which proceeds through the addition of benzylic Grignard reagents to the sulfinimine formed in situ from the condensation of 4-oxopiperidine-1-carboxylic acid *tert*-butyl ester and *N*-*tert*-butylsulfinamide.[47]

General Synthetic Chemistry Experimental Section. Reactions were carried out under N_2. Organic solutions were dried over $MgSO_4$ or Na_2SO_4. Starting materials and solvents were purchased from commercial suppliers and were used without further purification. Flash silica chromatography was performed using Merck silica gel 60 (0.025–0.04 mm). Ion exchange chromatography was performed using Isolute Flash SCX-II (acidic) or Flash NH2 (basic) resin cartridges. ^{1}H NMR spectra were recorded on Bruker AC250 or Bruker AMX500 instruments using internal deuterium locks. ^{13}C NMR spectra were recorded at 126 MHz on a Bruker AMX500 instrument using an internal deuterium lock. Chemical shifts (δ) are reported relative to TMS ($\delta = 0$) and/or referenced to the solvent in which they were measured. Combined HPLC−MS analyses were recorded using a Waters Alliance 2795 separations module and Waters/Micromass LCT mass detector with electrospray ionization (+ve or −ve ion mode as indicated) and with HPLC performed using a Supelco DISCOVERY C_{18} 5 cm × 4.6 mm i.d., 5 μm column, with gradient elution of 10−90% MeOH/0.1% aqueous formic acid at a flow rate of 1 mL min^{-1} and a run time of 6, 10, or 15 min as indicated. Compounds were detected at 254 nm using a Waters 2487 dual λ absorbance detector. Additional HPLC purities were determined on a Surveyor HPLC using a Phenomenex gemini 5 μm C_{18} 25 cm × 4.6 mm i.d. column, with gradient elution of 10−90% MeOH/0.1% aqueous formic acid at a flow rate of 1 mL min^{-1} and a run time of 10 min. High-resolution mass spectra were measured on an Agilent 6210 ToF MS with a Phenomenex Gemini 3 μm C_{18} (3 cm × 4.6 mm i.d) column. Synthetic intermediates were characterized by ^{1}H NMR spectra and MS (where electrospray ionization permitted observation of a relevant ion) for identity and were assessed by ^{1}H NMR for homogeneity. Key compounds for biological testing were additionally characterized by ^{13}C NMR and HRMS for identity and were assessed by HPLC (area-under-curve, UV detection) for homogeneity.

General Method for the Preparation of 6-(Piperidin-1-yl)-purines. (1-(9*H*-Purin-6-yl)piperidin-4-yl)methanamine (5). A solution of 6-chloropurine (**26**) (0.100 g, 0.646 mmol), *tert*-butyl piperidin-4-ylmethylcarbamate (0.277 mg, 1.29 mmol), and Et_3N (0.450 mL, 3.23 mmol) in *n*-BuOH (6.5 mL) was stirred at 100 °C for 15 h. The mixture was cooled and concentrated, and the residues were triturated with MeOH (10 mL). The white solid was collected and dried in vacuo to give *tert*-butyl (1-(9*H*-purin-6-yl)piperidin-4-yl)methylcarbamate (**27**) (0.124 mg, 0.373 mmol, 58%). LC−MS (15 min) *m*/*z* 333 [M + H$^+$], t_R = 5.42 min; ^{1}H NMR (500 MHz, DMSO) δ 12.95 (br s, 1H), 8.18 (s, 1H), 8.09 (s, 1H), 6.89–6.86 (m, 1H), 5.36 (br s, 2H), 3.04 (br s, 2H), 2.84 (t, J 6.0 Hz, 2H), 1.75–1.70 (m, 3H), 1.38 (s, 9H), 1.15–1.05 (m, 2H); ^{13}C NMR (DMSO) δ 155.8, 153.1, 151.8, 151.4, 137.8, 118.7, 77.4, 45.3, 44.5, 36.4, 29.6, 28.3 ppm. A solution of **27** (0.112 g, 0.337 mmol) in 2 M HCl (4 mL) was stirred at room temperature for 17 h. The solution was concentrated and the crude product was purified by ion exchange chromatography on acidic resin, eluting with MeOH and then 1 M NH_3−MeOH, to give **5** (0.078 g, 0.336 mmol, 99%). LC−MS (10 min) *m*/*z* 219 [M + H$^+$], t_R = 0.71 min, purity >98%; found [M + H$^+$] 219.1353, $C_{10}H_{15}N_6$ requires 219.1358; HPLC purity >98% AUC; ^{1}H NMR (250 MHz, MeOD) δ 8.20 (s, 1H), 8.00 (s, 1H), 5.47–5.42 (m, 2H), 3.13 (dt, *J* 13.0, 2.5 Hz, 2H), 2.60 (d, *J* 6.5 Hz, 2H), 1.96–1.89 (m, 2H), 1.85–1.71 (m, 1H), 1.27 (dq, *J* 13.0, 4.5 Hz, 2H); ^{13}C NMR (DMSO) δ 153.1, 151.7, 151.6, 138.0, 118.7, 47.4, 44.8, 39.1, 29.7 ppm.

General Method for the Preparation of 4-(Piperidin-1-yl)-1*H*-pyrazolo[3,4-*d*]pyrimidines. 1-(1*H*-Pyrazolo[3,4-*d*]pyrimidin-4-yl)piperidin-4-amine (8). A solution of 4-chloro-1*H*-pyrazolo[3,4-*d*]pyrimidine (**30**)[42] (0.059 g, 0.38 mmol), *tert*-butyl piperidin-4-ylcarbamate (0.134 g, 0.67 mmol), and Et_3N (0.100 mL, 0.72 mmol) in EtOH (2 mL) was stirred at 80 °C for 3 h. The solution was cooled and evaporated to dryness, and the residue was purified by recrystallization (^{i}PrOH) to give *tert*-butyl 1-(*1*H-pyrazolo[3,4-*d*]pyrimidin-4-yl)piperidin-4-ylcarbamate (0.032 g, 26%). ^{1}H NMR (250 MHz, $CDCl_3$) δ 8.46 (1H, s), 8.06 (1H, s), 4.75 (2H, d, *J* 12 Hz), 4.55 (1H, d, *J* 8 Hz), 3.90–3.80 (1H, m), 3.37 (2H, dd, *J* = 12, 12 Hz), 2.21–2.17 (2H, m), 1.62–1.43 (2H, m), 1.49 (9H, s). HCl (4 M) in dioxane (1 mL, 4 mmol) was added to a portion of the material (0.028 g, 0.088 mmol). The suspension was stirred at room temperature for 1 h and then diluted with Et_2O (4 mL). The precipitate was washed with Et_2O, and the solid was collected and dried in vacuo. Purification by ion exchange chromatography on SCXII acidic resin, eluting with MeOH and then 2 M NH_3−MeOH, gave **8** (0.011 g, 57%). LC−MS (15 min) *m*/*z* 219 [M + H$^+$], t_R = 0.86 min, purity 95%; ^{1}H NMR (250 MHz, DMSO) δ 8.30 (1H, s), 8.23 (1H, s), 4.75–4.50 (1H, m), 4.00–3.10 (4H, m), 1.95 (2H, d, *J* 12 Hz), 1.50–1.20 (2H, m); ^{13}C NMR (DMSO) δ 156.1, 155.6, 154.7, 133.5, 99.2, 47.4, 39.8, 30.0 ppm.

General Method for the Preparation of 4-(Piperidin-1-yl)-7*H*-pyrrolo[2,3-*d*]pyrimidines. 1-(7*H*-Pyrrolo[2,3-*d*]pyrimidin-4-yl)piperidin-4-amine (10). A solution of 4-chloro-7*H*-pyrrolo[2,3-*d*]pyrimidine (**31**)[48] (0.074 g, 0.48 mmol), *tert*-butyl piperidin-4-ylcarbamate (0.106 g, 0.53 mmol), and Et_3N (0.20 mL, 1.43 mmol) in EtOH (1 mL) was heated at 80 °C for 4 h. The mixture was cooled to room temperature and the resulting precipitate was collected and washed with EtOH (2 mL), then dried in vacuo to give *tert*-butyl 1-(7*H*-pyrrolo[2,3-*d*]pyrimidin-4-yl)piperidin-4-ylcarbamate (0.057 g, 0.180 mmol, 38%). LC−MS (15 min) *m*/*z* 318 [M + H$^+$], t_R = 4.57 min; ^{1}H NMR (250 MHz, $CDCl_3$) δ 9.60 (1H, br s), 8.35 (1H, s), 7.09 (1H, d, *J* 3 Hz), 6.54 (1H, d, *J* = 3 Hz), 4.75–4.69 (2H, m), 4.50–4.45 (1H, m), 3.90–3.70 (1H, m), 3.29 (2H, ddd, *J* = 12, 12, 5 Hz), 2.15–2.11 (2H, m), 1.58–1.45 (2H, m), 1.49 (9H, s). A solution of the material in 4 M HCl−dioxane (1 mL, 4 mmol) was stirred at room temperature for 1 h and then diluted with Et_2O (4 mL). The resulting precipitate was washed with Et_2O and dried in vacuo to give **10**, hydrochloride salt (0.027 g, 0.107 mmol, 59%). A sample of the free base was prepared by ion exchange chromatography on SCXII acidic resin, eluting with 1 M NH_3−MeOH. LC−MS (15 min) *m*/*z* 218 [M + H$^+$], t_R = 0.81 min, purity >98%; ^{1}H NMR (250 MHz, DMSO) δ 12.82 (1H, s), 8.40 (1H, s), 8.31 (2H, br s), 7.51 (1H, br s), 7.00 (1H, br s), 4.65 (2H, d, *J* 12 Hz), 3.53–3.35 (3H, m), 2.17 (2H, d, *J* 10 Hz), 1.80–1.60 (2H, m); ^{13}C NMR (MeOD) δ 158.3, 152.5, 151.7, 122.3, 104.2, 102.5, 46.2, 35.7 ppm.

General Method for the Preparation of 4-(Piperidin-1-yl)-1*H*-pyrrolo[2,3-*b*]pyridines. 1-(1*H*-Pyrrolo[2,3-*b*]pyridin-4-yl)piperidin-4-amine (12). A mixture of 4-chloro-1*H*-pyrrolo[2,3-*b*]pyridine (**32**)[43] (0.10 g, 0.64 mmol), *tert*-butyl piperidin-4-ylcarbamate (0.453 g, 2.24 mmol), and *N*-methylpyrrolidinone (0.2 mL) was heated at 160 °C in a microwave reactor for 1 h. The cooled solution was diluted with MeOH and purified by ion exchange on SCXII acidic resin, eluting with MeOH and then with 3 M NH_3−MeOH. The crude product was further purified by flash silica column chromatography, eluting with 8% MeOH−CH_2Cl_2, to give *tert*-butyl 1-(1*H*-pyrrolo[2,3-*b*]pyridin-4-yl)piperidin-4-ylcarbamate (0.56 g, 0.18 mmol, 28%). LC−MS (15 min) *m*/*z* 316 [M]$^+$, t_R = 4.64 min; ^{1}H NMR (250 MHz, MeOD) δ 7.94–7.92 (d, *J* = 5 Hz, 1H), 7.20–7.18 (d, *J* = 5 Hz, 1H), 6.52–6.49 (m, 2H), 4.08–4.03 (m, 2H), 3.70–3.55 (m, 1H), 3.15–3.05 (m, 2H),

2.05–2.01 (m, 2H), 1.74–1.64 (m, 2H), 1.48 (s, 9H). CF_3CO_2H (1 mL) was added dropwise to a portion of the material (0.19 g, 0.06 mmol) dissolved in CH_2Cl_2 (1 mL) and stirred at 0 °C. After 2.5 h solvents were removed by evaporation and the crude product was purified by ion exchange on NH_2 basic resin, eluting with MeOH, to give **12** (0.013 mg, 0.058 mmol, 96%). LC−MS (15 min) *m/z* 217 [M + H]$^+$, t_R = 0.95 min, purity 90%; ^{1}H NMR (250 MHz, MeOD) δ 8.15–8.13 (d, *J* = 5 Hz, 1H), 7.20–7.18 (d, *J* = 5 Hz, 1H), 6.53–6.50 (m, 2H), 4.12–4.07 (m, 2H), 3.09–2.91 (m, 2H), 2.03–2.00 (m, 2H), 1.68–1.54 (m, 3H); ^{13}C NMR (MeOD) δ 153.3, 150.6, 144.4, 131.9, 123.1, 117.1, 112.0, 102.9, 101.2, 49.5, 35.3 ppm.

***C*-(4-Chlorophenyl)-*C*-[1-(7*H*-pyrrolo[2,3-*d*]pyrimidin-4-yl)piperidin-4-yl]methylamine (14).** Boc_2O (1.00 g, 4.59 mmol) was added at room temperature to a stirred mixture of (4-chlorophenyl)piperidin-4-ylmethanone hydrochloride (**33**) (0.996 g, 3.83 mmol) and Et_3N (2.7 mL, 19.1 mmol) in MeCN (15 mL). After 16 h the mixture was evaporated to dryness and partitioned between EtOAc (50 mL) and 1 M HCl (20 mL). The organic phase was separated and washed successively with saturated aqueous $NaHCO_3$ (20 mL) and brine (20 mL), then dried and evaporated to dryness. Flash silica column chromatography, eluting with 60% Et_2O−hexane, gave *tert*-butyl 4-(4-chlorobenzoyl)piperidine-1-carboxylate as an oil (1.12 g, 3.48 mmol, 91%). LC−MS (15 min) *m/z* 346 [M + Na$^+$], t_R = 7.42 min; ^{1}H NMR (250 MHz, $CDCl_3$) δ 7.93–7.87 (m, 2H), 7.50–7.45 (m, 2H), 4.22–4.16 (m, 2H), 3.44–3.32 (m, 1H), 2.98–2.86 (m, 2H), 1.89–1.68 (m, 4H), 1.49 (s, 9H). $NaCNBH_3$ (0.866 g, 13.8 mmol) was added at room temperature to a stirred mixture of *tert*-butyl 4-(4-chlorobenzoyl)piperidine-1-carboxylate (1.12 g, 3.48 mmol) and ammonium acetate (3.19 g, 41.4 mmol) in MeOH (34 mL). After refluxing for 20 h the mixture was cooled, concentrated, and stirred with 1 M NaOH aq (100 mL). The aqueous phase was extracted with Et_2O (3 × 75 mL). The combined organic extracts were dried, filtered and concentrated. Flash silica column chromatography, eluting with 15% MeOH−CH_2Cl_2, gave 4-(amino-(4-chlorophenyl)methyl)piperidine-1-carboxylic acid *tert*-butyl ester (0.913 g, 2.85 mmol, 82%). LC−MS (15 min) *m/z* 208 [M − Boc − NH_2^+], t_R = 5.56 min; ^{1}H NMR (250 MHz, $CDCl_3$) δ 7.35–7.22 (m, 4H), 4.22–4.03 (m, 2H), 3.65 (d, *J* 7.5 Hz, 1H), 2.73–2.53 (m, 2H), 1.94–1.87 (m, 1H), 1.65–1.54 (m, 1H), 1.46 (s, 9H), 1.34–0.98 (m, 3H). HCl (2 M, 6 mL) was added at room temperature to a solution of 4-[amino-(4-chlorophenyl)methyl]piperidine-1-carboxylic acid *tert*-butyl ester (0.192 g, 0.591 mmol) in MeOH (6 mL). After being stirred for 16 h, the solution was evaporated to dryness to give *C*-(4-chlorophenyl)-*C*-piperidin-4-ylmethylamine dihydrochloride (**34a**) (0.174 g, 0.583 mmol, 99%) as a white foam. LC−MS (6 min) *m/z* 208 [M − NH_2^+], t_R = 0.56 min; ^{1}H NMR (250 MHz, MeOD) δ 7.61–7.53 (4H, m), 4.22 (1H, d, 9.5 Hz), 3.61–3.35 (2H, m), 3.17–2.90 (2H, m), 2.50–2.22 (2H, m), 1.82–1.40 (2H, m); ^{13}C NMR (MeOD) δ 136.6, 135.4, 130,7, 130.6, 60.0, 44.5, 44.4, 38.8, 27.0, 26.4 ppm. A solution of **34a** (0.050 g, 0.168 mmol), **31** (0.026 g, 0.168 mmol), and Et_3N (0.117 mL, 0.840 mmol) in *n*-BuOH (1.7 mL) was heated at 100 °C for 48 h. The mixture was concentrated and purified by ion exchange chromatography on NH_2 basic resin, eluting with MeOH. Flash silica column chromatography, eluting with 15% MeOH−CH_2Cl_2, gave **14** (30 mg, 0.088 mmol, 52%) as an off-white solid. LC−MS (6 min) *m/z* 342 [M + H$^+$], t_R = 1.84 min, purity >98%; found [M + H$^+$] 342.1473, $C_{18}H_{21}N_5Cl$ requires 342.1485; HPLC purity >98%; ^{1}H NMR (250 MHz, MeOD) δ 8.12 (s, 1H), 7.38–7.31 (m, 4H), 7.11 (s, *J* = 3.5 Hz, 1H), 6.59 (s, *J* = 3.5 Hz, 1H), 4.95–4.65 (m, 2H), 3.60 (d, *J* = 8.5 Hz, 1H), 3.18–2.95 (m, 2H), 2.16–2.08 (m, 1H), 1.99–1.85 (m, 1H), 1.47–1.16 (m, 3H); ^{13}C NMR (MeOD) δ 158.2, 152.4, 151.7, 143.8, 134.0, 131.2, 130.15, 130.0, 129.6, 122.2, 61.5, 47.3, 47.2, 44.7, 30.5, 30.2 ppm.

***C*-(4-(4-Chlorophenyl)-1-(7*H*-pyrrolo[2,3-*d*]pyrimidin-4-yl)piperidin-4-yl)methylamine (18).** NaH (60% dispersion in mineral oil, 2.90 g, 72.3 mmol) was added in small portions over 1 h to a solution of bis-(2-chloroethyl)carbamic acid *tert*-butyl ester[45] (6.74 g, 28.0 mmol) and 4-chlorobenzyl cyanide (**35**) (3.80 g, 25 mmol) in anhydrous DMF (25 mL). The reaction mixture was heated at 65 °C for 1 h and then stirred at room temperature for 89 h. The reaction mixture was poured into ice–water (60 mL) and extracted with EtOAc (2 × 100 mL). The combined organic extracts were washed with water and brine, dried, filtered, and concentrated. Flash silica column chromatography, eluting with hexane−CH_2Cl_2−EtOAc (8:1:1), gave 4-(4-chlorophenyl)-4-cyanopiperidin-1-carboxylic acid *tert*-butyl ester[46] (**36**) (5.60 g, 17.5 mmol, 70%) as a white solid. LC−MS (15 min) *m/z* 320 [M $^+$], t_R = 7.71 min; ^{1}H NMR (250 MHz, $CDCl_3$) δ 7.43–7.41 (m, 4H), 4.31 (br d, *J* = 13 Hz, 2H), 3.22 (br t, *J* = 13 Hz, 2H), 2.14–2.05 (m, 2H), 1.93 (dt, *J* = 13, 4.5 Hz, 2H), 1.51 (s, 9H); ^{13}C NMR ($CDCl_3$) δ 154.4, 138.2, 134.4, 129.3, 127.0, 121.0, 80.3, 42.6, 41.2 (br), 36.2, 28.4 ppm. Raney nickel (Raney nickel suspension 2800, 1 mL) was added at room temperature to a stirred solution of **36** (0.355 g, 1.11 mmol) in EtOH (20 mL), and the suspension was stirred under H_2 (1 atm) for 20 h. The suspension was filtered through Celite, and the filtrate was concentrated to give 4-aminomethyl-4-(4-chlorophenyl)piperidine-1-carboxylic acid *tert*-butyl ester (0.258 g, 0.794 mmol, 72%) as an oil. LC−MS (15 min) *m/z* 324 [M − ^{t}Bu − NH_2^+], t_R = 5.02 min; ^{1}H NMR (250 MHz, $CDCl_3$) δ 7.40–7.35 (m, 2H), 7.28–7.24 (m, 2H), 3.80–3.70 (m, 2H), 3.06 (ddd, *J* = 13.5, 10.5, 3.0 Hz, 2H), 2.78 (s, 2H), 2.20–2.12 (m, 2H), 1.72 (ddd, *J* = 14.0, 10.5, 4.0 Hz, 2H), 1.47 (s, 9H). HCl (2 M, 10 mL) was added at room temperature to a solution of 4-aminomethyl-4-(4-chlorophenyl)piperidine-1-carboxylic acid *tert*-butyl ester (0.258 g, 0.794 mmol) in MeOH (10 mL). After 18 h the solution was concentrated to dryness to give *C*-(4-(4-chlorophenyl)piperidin-4-yl)methylamine hydrochloride (**37**) (0.232 g, 0.778 mmol, 98%). LC−MS (6 min) *m/z* 324 [M − ^{t}Bu − NH_2^+], t_R = 0.59 min; ^{1}H NMR (250 MHz, MeOD) δ 7.59–7.51 (4H, m), 3.46–3.37 (2H, m), 3.24 (2H, s), 3.02–2.92 (2H, m), 2.66–2.60 (2H, m), 2.22–2.10 (2H, m); ^{13}C NMR (MeOD) determined as the free base δ 143.7, 133.2, 130.2, 129.8, 54.6, 43.2, 43.1, 34.5 ppm. A solution of **37** (0.060 g, 0.202 mmol), **31** (0.031 g, 0.202 mmol), and Et_3N (0.14 mL, 1.01 mmol) in *n*-BuOH (2 mL) was heated at 100 °C for 48 h. The reaction mixture was evaporated to dryness and purified by ion exchange chromatography on SCX-II acidic resin, eluting with MeOH and then 1 M NH_3−MeOH, to give the crude amine. Flash silica column chromatography, eluting with 15−20% MeOH−CH_2Cl_2, gave **18** (0.018 g, 0.053 mmol, 26%) as an off-white foam. LC−MS (10 min) *m/z* 342 [M + H$^+$], t_R = 2.70 min, purity 93%; found [M + H$^+$] 342.1485, $C_{18}H_{21}N_5Cl$ requires 342.1485; HPLC purity 90%; ^{1}H NMR (500 MHz, MeOD) δ 8.12 (s, 1H), 7.50–7.44 (m, 4H), 7.12 (d, *J* = 3.5 Hz, 1H), 6.63 (d, *J* = 3.5 Hz, 1H), 4.38 (dt, *J* = 13.5, 4.5 Hz, 2H), 3.49 (ddd, *J* = 13.5, 10.5, 3.0 Hz, 2H), 2.84 (s, 2H), 2.40–2.35 (m, 2H), 1.95–1.90 (m, 2H); ^{13}C NMR (MeOD) δ 158.3, 152.4, 151.6, 142.6, 133.7, 130.3, 130.1, 122.3, 104.3, 102.6, 53.7, 43.7, 43.1, 33.9 ppm.

4-(4-Chlorobenzyl)-1-(7*H*-pyrrolo[2,3-*d*]pyrimidin-4-yl)piperidin-4-ylamine (25). *n*-BuLi (36.2 mL, 2.3 M solution in hexanes, 84 mmol) was added at −78 °C to a solution of ^{i}Pr$_2$NH (11.8 mL, 84 mmol) in THF (230 mL). After 10 min a solution of 4-cyanopiperidine-1-carboxylic acid *tert*-butyl ester (**40**)[49] (15.4 g, 73.1 mmol) in THF (92 mL) was added at −78 °C. After 1 h a solution of 4-chlorobenzyl chloride (11.1 mL, 88 mmol) in THF (40 mL) was added and the solution was warmed to room temperature over 15 h. Water (500 mL) was added, and the mixture was extracted with Et_2O (500 mL). The organic extract was dried and concentrated to give a solid. Recrystallization from Et_2O−hexane gave 4-(4-chlorobenzyl)-4-cyanopiperidine-1-carboxylic acid *tert*-butyl ester (**41**) (11.0 g, 32.3 mmol, 44%) as a white solid. LC−MS (10 min) *m/z* 357 [M + Na$^+$], 235 [M − Boc]$^+$, t_R = 8.02 min; ^{1}H NMR ($CDCl_3$) δ 7.35–7.32 (m, 2H), 7.24–7.21 (m, 2H), 4.15 (br s, 2H), 3.00 (br t, *J* = 12.0 Hz, 2H), 2.84 (s, 2H), 1.84 (br d, *J* = 13.0 Hz, 2H), 1.52–1.46 (m, 2H), 1.47 (s, 9H); ^{13}C NMR ($CDCl_3$) δ 154.4, 133.7, 132.7, 131.5, 128.7, 121.6, 80.1, 45.2, 40.9 (br), 39.1, 34.7, 28.4 ppm. A solution of **41** (6 g, 17.9 mmol) in 9 M HCl (180 mL) was refluxed for 3 days. Additional 12 M HCl (100 mL) was added, and reflux was continued for 2 days. The solution was evaporated to dryness, then diluted with 2 M NaOH (360 mL). Boc_2O (4.69 g, 21.5 mmol) was added, and the mixture was stirred

at room temperature for 24 h. The acidity was adjusted to pH 6 using 2 M HCl, and the mixture was extracted with Et_2O (2 × 200 mL). The extracts were concentrated. Flash column chromatography, eluting with 5% MeOH−CH_2Cl_2, gave 1-(*tert*-butoxycarbonyl)-4-(4-chlorobenzyl)piperidine-4-carboxylic acid (**43**) (4.29 g, 68%). LC−MS (15 min) *m/z* 376 [M + Na^+], t_R = 7.62 min; ^{1}H NMR (500 MHz, MeOD) δ 7.28–7.25 (m, 2H), 7.16–7.13 (m, 2H), 3.92 (dt, *J* 13.5, 3.5 Hz, 2H), 2.92 (br s, 2H), 2.85 (s, 2H), 2.03 (br d, *J* = 13.5 Hz, 2H), 1.46 (s, 9H), 1.45–1.39 (m, 2H); ^{13}C NMR (MeOD) δ 178.5, 156.6, 136.9, 133.6, 132.7, 129.1, 81.0, 48.3, 46.5, 42.7 (br), 34.4, 28.7 ppm. Isobutyl chloroformate (0.812 mL, 6.19 mmol) was added at −15 °C to a mixture of **43** (1.46 g, 4.13 mmol) and Et_3N (1.15 mL, 8.25 mmol) in THF (41 mL). After 1 h a solution of NaN_3 (0.536 g, 8.25 mmol) in water (10 mL) was added and the solution was warmed to room temperature overnight. Water (100 mL) was added, and the mixture was extracted with Et_2O (3 × 50 mL). The organic extracts were combined, washed with saturated aqueous $NaHCO_3$ (50 mL), and dried. Toluene (100 mL) was added, and the overall volume was reduced by evaporation to approximately 90 mL. The solution was warmed to 90 °C for 2 h, then cooled and poured into 10% HCl (70 mL). The biphasic mixture was warmed to 90 °C for 24 h. The organic phase was separated and concentrated to dryness to give the crude amine salt (1.11 g). The material was dissolved in 2 M NaOH (20 mL), and Boc_2O (1.61 g, 7.39 mmol) was added. After 2 days the mixture was extracted with Et_2O (2 × 50 mL). The organic extracts were combined, washed with 1 M HCl (20 mL), saturated aqueous $NaHCO_3$ (20 mL), and brine (20 mL), then dried and concentrated. Flash silica column chromatography, eluting with 50% Et_2O−hexane, gave the doubly Boc-protected amine (0.685 g), which was deprotected by stirring with 4 M HCl in dioxane (10 mL) and MeOH (10 mL) at room temperature for 2 days. Concentration of the solution gave 4-(4-chlorobenzyl)piperidin-4-yl amine hydrochloride (**44**) (0.492 g, 1.65 mmol, 40% from **43**). LC−MS (10 min) *m/z* 208 [M − NH_2^+], t_R = 0.60 min; ^{1}H NMR (500 MHz, MeOD) δ 7.44 (d, *J* = 8.5 Hz, 2H), 7.33 (d, *J* = 8.5 Hz, 2H), 3.49–3.46 (m, 4H), 3.20 (s, 2H), 2.16–2.13 (m, 4H); ^{13}C NMR (MeOD) δ 135.3, 133.6, 133.0, 130.3, 54.4, 41.2, 40.6, 31.0 ppm. A solution of **44** (0.060 g, 0.202 mmol), **31** (0.031 g, 0.202 mmol), and Et_3N (0.140 mL, 1.01 mmol) in *n*-BuOH (2.0 mL) was heated at 100 °C for 24 h. The mixture was concentrated and purified by preparative silica TLC, eluting with 10% MeOH−CH_2Cl_2, to give **25** (0.034 g, 49%). Recrystallization from MeOH gave a white powder, mp 214–216 °C. LC−MS (10 min) *m/z* 342 [M + H^+], t_R = 2.75 min, purity >98%; found [M + H^+] 342.1494, $C_{18}H_{21}N_5Cl$ requires 342.1485; HPLC purity >98%; ^{1}H NMR (MeOD) δ 8.12 (s, 1H), 7.33–7.30 (m, 2H), 7.24–7.22 (m, 2H), 7.11 (d, *J* = 3.5 Hz, 1H), 6.61 (d, *J* = 3.5 Hz, 1H), 4.28 (dt, *J* = 14.0, 5.0 Hz, 2H), 3.78 (ddd, *J* = 14.0, 10.0, 3.0 Hz, 2H), 2.78 (s, 2H), 1.75 (ddd, *J* = 14.0, 10.0, 4.0 Hz, 2H), 1.57–1.53 (m, 2H); ^{13}C NMR (MeOD) δ 158.3, 152.4, 151.7, 136.9, 133.6, 133.4, 129.3, 122.2, 104.2, 102.6, 51.4, 48.7, 43.2, 38.2 ppm.

Acknowledgment. This work was supported by Cancer Research UK [CUK] Grant No. C309/A2187. The authors thank B. Graham and S. Saalau-Bethell for protein purification, W. Blakemore for assistance with PKA−PKB crystallography, and A. Mirza and M. Richards for assistance with compound characterization.

Supporting Information Available: Details of the X-ray crystallography data collection and refinement (**5**−PKA−PKB, **6**−PKA−PKB, **18**−PKA−PKB, **21**−PKA−PKB, **25**−PKA−PKB, **25**−PKA); detailed results of the search for S···NH_3^+ contacts in the Cambridge Structural Database; HPLC purities of key compounds; experimental procedures for PKBβ and PKA biochemical assays; experimental procedures for SRB and ELISA cellular assays; experimental procedures for the measurement of in vivo PK properties (**25**); synthetic procedures and characterization of compounds **3**, **4**, **6**, **7**, **9**, **11**, **13**, **15**–**17**, **19**–**24**, **28**, **38**, **39**, and **42**. This material is available free of charge via the Internet at http://pubs.acs.org.

References

(1) Hennessy, B. T.; Smith, D. L.; Ram, P. T.; Lu, Y.; Mills, G. B. Exploiting the PI3K/AKT pathway for cancer drug discovery. *Nat. Rev. Drug Discovery* **2005**, *4*, 988–1004.
(2) Georgiakis, G. V.; Younes, A. From Rapa Nui to rapamycin: targeting PI3K/Akt/mTOR for cancer therapy. *Expert Rev. Anticancer Ther.* **2006**, *6*, 131–140.
(3) Cheng, J. Q.; Lindsley, C. W.; Cheng, G. Z.; Yang, H.; Nicosia, S. V. The Akt/PKB pathway: molecular target for cancer drug discovery. *Oncogene* **2005**, *24*, 7482–7492.
(4) Cully, M.; You, H.; Levine, A. J.; Mak, T. W. Beyond PTEN mutations: the PI3K pathway as an integrator of multiple inputs during tumorigenesis. *Nat. Rev. Cancer* **2006**, *6*, 184–192.
(5) Tokunaga, E.; Kimura, Y.; Oki, E.; Ueda, N.; Futatsugi, M.; Mashino, K.; Yamamoto, M.; Ikebe, M.; Kakeji, Y.; Baba, H.; Maehara, Y. Akt is frequently activated in HER2/neu-positive breast cancers and associated with poor prognosis among hormone-treated patients. *Int. J. Cancer.* **2006**, *118*, 284–289.
(6) Bader, A. G.; Khang, S.; Zhao, L.; Vogt, P. K. Oncogenic PI3K deregulates transcription and translation. *Nat. Rev. Cancer* **2005**, *5*, 921–929.
(7) Leslie, N. R.; Downes, C. P. PTEN function: how normal cells control it and tumour cells lose it. *Biochem. J.* **2004**, *382*, 1–11.
(8) Testa, J. R.; Bellacosa, A. AKT plays a central role in tumorigenesis. *Proc. Natl. Acad. Sci U.S.A.* **2001**, *98*, 10983–10985.
(9) (a) Fan, Q. W.; Knight, Z. A.; Goldenberg, D. D.; Yu, W.; Mostov, K. E.; Stokoe, D.; Shokat, K. M.; Weiss, W. A. A dual PI3 kinase/mTOR inhibitor reveals emergent efficacy in glioma. *Cancer Cell* **2006**, *9*, 341–349. (b) Raynaud, F. I.; Eccles, S.; Clarke, P. A.; Hayes, A.; Nutley, B.; Alix, S.; Henley, A.; Di-Stefano, F.; Ahmad, Z.; Guillard, S.; Bjerke, L. M.; Kelland, L.; Valenti, M.; Patterson, L.; Gowan, S.; de Haven Brandon, A.; Hayakawa, M.; Kaizawa, H.; Koizumi, T.; Ohishi, T.; Patel, S.; Saghir, N.; Parker, P.; Waterfield, M.; Workman, P. Pharmacologic characterization of a potent inhibitor of class I phosphatidylinositide 3-kinases. *Cancer Res.* **2007**, *67*, 5840–5850.
(10) Luo, Y.; Shoemaker, A. R.; Liu, X.; Woods, K. W.; Thomas, S. A.; de Jong, R.; Han, E. K.; Li, T.; Stoll, V. S.; Powlas, J. A.; Oleksijew, A.; Mitten, M. J.; Shi, Y.; Guan, R.; McGonigal, T. P.; Klinghofer, V.; Johnson, E. F.; Leverson, J. D.; Bouska, J. J.; Mamo, M.; Smith, R. A.; Gramling-Evans, E. E.; Zinker, B. A.; Mika, A. K.; Nguyen, P. T.; Oltersdorf, T.; Rosenberg, S. H.; Li, Q.; Giranda, V. L. Potent and selective inhibitors of Akt kinases slow the progress of tumors in vivo. *Mol. Cancer Ther.* **2005**, *4*, 977–986.
(11) Barnett, S. F.; Bilodeau, M. T.; Lindsley, C. W. The Akt/PKB family of protein kinases: a review of small molecule inhibitors and progression towards target validation. *Curr. Top. Med. Chem.* **2005**, *5*, 109–125.
(12) Collins, I.; Workman, P. New approaches to molecular cancer therapeutics. *Nat. Chem. Biol.* **2006**, *2*, 689–700.
(13) Workman, P.; Clarke, P. A.; Guillard, S.; Raynaud, F. I. Drugging the PI3 kinome. *Nat. Biotechnol.* **2006**, *24*, 794–796.
(14) (a) Woods, K. W.; Fischer, J. P.; Claiborne, A.; Li, T.; Thomas, S. A.; Zhu, G.; Diebold, R. B.; Liu, X.; Shi, Y.; Klinghofer, V.; Han, E. K.; Guan, R.; Magnone, S. R.; Johnson, E. F.; Bouska, J. J.; Olson, A. M.; de Jong, R.; Oltersdorf, T.; Luo, Y.; Rosenberg, S. H.; Giranda, V. L.; Li, Q. Synthesis and SAR of indazole-pyridine based protein kinase B/Akt inhibitors. *Bioorg. Med. Chem.* **2006**, *14*, 6832–6846. (b) Li, Q; Woods, K. W.; Thomas, S.; Zhu, G. D.; Packard, G.; Fisher, J.; Li, T.; Gong, J.; Dinges, J.; Song, X.; Abrams, J.; Luo, Y.; Johnson, E. F.; Shi, Y.; Liu, X.; Klinghofer, V.; Des Jong, R.; Oltersdorf, T.; Stoll, V. S.; Jakob, C. G.; Rosenberg, S. H.; Giranda, V. L. Synthesis and structure−activity relationship of 3,4′-bispyridinylethylenes: discovery of a potent 3-isoquinolinylpyridine inhibitor of protein kinase B (PKB/Akt) for the treatment of cancer. *Bioorg. Med. Chem. Lett.* **2006**, *16*, 2000–2007. (c) Zhu, G. D.; Gong, J.; Claiborne, A.; Woods, K. W.; Gandhi, V. B.; Thomas, S.; Luo, Y.; Liu, X.; Shi, Y.; Guan, R.; Magnone, S. R.; Klinghofer, V.; Johnson, E. F.; Bouska, J.; Shoemaker, A.; Oleksijew, A.; Stoll, V. S.; De Jong, R.; Oltersdorf, T.; Li, Q.; Rosenberg, S. H.; Giranda, V. L. Isoquinoline-pyridine-based protein kinase B/Akt antagonists: SAR and in vivo antitumor activity. *Bioorg. Med. Chem. Lett.* **2006**, *16*, 3150–3155. (d) Zhu, G. D.; Gandhi, V. B.; Gong, J.; Luo, Y.; Liu, X.; Shi, Y.; Guan, R.; Magnone, S. R.; Klinghofer, V.; Johnson, E. F.; Bouska, J.; Shoemaker, A.; Oleksijew, A.; Jarvis, K.; Park, C.; Jong, R. D.; Oltersdorf, T.; Li, Q.; Rosenberg, S. H.; Giranda, V. L. Discovery and SAR of oxindole-pyridine-based protein kinase B/Akt inhibitors for treating cancers. *Bioorg. Med. Chem. Lett.* **2006**, *16*, 3424–3429. (e) Thomas,

S. A.; Li, T.; Woods, K. W.; Song, X.; Packard, G.; Fischer, J. P.; Diebold, R. B.; Liu, X.; Shi, Y.; Klinghofer, V.; Johnson, E. F.; Bouska, J. J.; Olson, A.; Guan, R.; Magnone, S. R.; Marsh, K.; Luo, Y.; Rosenberg, S. H.; Giranda, V. L.; Li, Q. Identification of a novel 3,5-disubstituted pyridine as a potent, selective, and orally active inhibitor of Akt1 kinase. *Bioorg. Med. Chem. Lett.* **2006**, *16*, 3740–3704. (f) Zhu, G. D.; Gong, J.; Gandhi, V. B.; Woods, K.; Luo, Y.; Liu, X.; Guan, R.; Klinghofer, V.; Johnson, E. F.; Stoll, V. S.; Mamo, M.; Li, Q.; Rosenberg, S. H.; Giranda, V. L. Design and synthesis of pyridine-pyrazolopyridine-based inhibitors of protein kinase B/Akt. *Bioorg. Med. Chem.* **2007**, *15*, 2441–2452. (g) Zhu, G. D.; Gandhi, V. B.; Gong, J.; Thomas, S.; Woods, K. W.; Song, X.; Li, T.; Diebold, R. B.; Luo, Y.; Liu, X.; Guan, R.; Klinghofer, V.; Johnson, E. F.; Bouska, J.; Olson, A.; Marsh, K. C.; Stoll, V. S.; Mamo, M.; Polakowski, J.; Campbell, T. J.; Martin, R. L.; Gintant, G. A.; Penning, T. D.; Li, Q.; Rosenberg, S. H.; Giranda, V. L. Syntheses of potent, selective, and orally bioavailable indazole-pyridine series of protein kinase B/Akt inhibitors with reduced hypotension. *J. Med. Chem.* **2007**, *50*, 2990–3003.

(15) (a) Breitenlechner, C. B.; Wegge, T.; Berillon, L.; Graul, K.; Marzenell, K.; Friebe, W. G.; Thomas, U.; Schumacher, R.; Huber, R.; Engh, R. A.; Masjost, B. Structure-based optimization of novel azepane derivatives as PKB inhibitors. *J. Med. Chem.* **2004**, *47*, 1375–1390. (b) Breitenlechner, C. B.; Friebe, W. G.; Brunet, E.; Werner, G.; Graul, K.; Thomas, U.; Kunkele, K. P.; Schafer, W.; Gassel, M.; Bossemeyer, D.; Huber, R.; Engh, R. A.; Masjost, B. Design and crystal structures of protein kinase B-selective inhibitors in complex with protein kinase A and mutants. *J. Med. Chem.* **2005**, *48*, 163–170.

(16) Ko, J. H.; Yeon, S. W.; Ryu, J. S.; Kim, T. Y.; Song, E. H.; You, H. J.; Park, R. E.; Ryu, C. K. Synthesis and biological evaluation of 5-arylamino-6-chloro-1*H*-indazole-4,7-diones as inhibitors of protein kinase B/Akt. *Bioorg. Med. Chem. Lett.* **2006**, *16*, 6001–6005.

(17) Burns, S.; Travers, J.; Collins, I.; Rowlands, M. G.; Newbatt, Y.; Thompson, N.; Garrett, M. D.; Workman, P.; Aherne, G. W. Identification of small molecule inhibitors of protein kinase B (PKB) in an AlphaScreen high-throughput screen. *J. Biomol. Screening* **2006**, *11*, 822–827.

(18) Collins, I.; Caldwell, J.; Fonseca, T.; Donald, A.; Bavetsias, V.; Rowlands, M. G.; Hunter, L.-J. K.; Garrett, M. D.; Davies, T. G.; Berdini, V.; Woodhead, S.; Davis, D.; Seavers, L. C. A.; Wyatt, P. G.; McDonald, E. Structure-based design of isoquinoline-5-sulfonamide inhibitors of protein kinase B. *Bioorg. Med. Chem.* **2006**, *14*, 1255–1273.

(19) Reuveni, H.; Livnah, N.; Geiger, T.; Klein, S.; Ohne, O.; Cohen, I.; Benhar, M.; Gellerman, G.; Levitski, A. Toward a PKB inhibitor: modification of a selective PKA inhibitor by rational design. *Biochemistry* **2002**, *41*, 10304–10314.

(20) Donald, A.; McHardy, T.; Rowlands, M. G.; Hunter, L-J. K.; Davies, T. G.; Berdini, V.; Boyle, R. G.; Aherne, G. W.; Garrett, M. D.; Collins, I. Rapid evolution of 6-phenylpurine inhibitors of protein kinase B through structure-based design. *J. Med. Chem.* **2007**, *50*, 2289–2292.

(21) Saxty, G.; Woodhead, S. J.; Berdini, V.; Davies, T. G.; Verdonk, M. L.; Wyatt, P. G.; Boyle, R. G.; Barford, D.; Downham, R.; Garrett, M. D.; Carr, R. A. Identification of novel inhibitors of protein kinase B using fragment-based lead discovery. *J. Med. Chem.* **2007**, *50*, 2293–2296.

(22) Gassell, M.; Breitenlechner, C. B.; Ruger, P.; Jucknischke, U.; Schneider, T.; Huber, R.; Bossemeyer, D.; Engh, R. A. Mutants of protein kinase A that mimic the ATP-binding site of protein kinase B (AKT). *J. Mol. Biol.* **2003**, *329*, 1021–1034.

(23) Davies, T. G.; Verdonk, M. L.; Graham, B.; Saalau-Bethell, S.; Hamlett, C. C.; McHardy, T.; Collins, I.; Garrett, M. D.; Workman, P.; Woodhead, S. J.; Jhoti, H.; Barford, D. A structural comparison of inhibitor binding to PKB, PKA and PKA−PKB chimera. *J. Mol. Biol.* **2007**, *367*, 882–894.

(24) Hopkins, A. L.; Groom, C. R.; Alex, A. Ligand efficiency: a useful metric for lead selection. *Drug Discovery Today* **2004**, *9*, 430–431.

(25) Yang, J.; Cron, P.; Good, V. M.; Thompson, V.; Hemmings, B. A.; Barford, D. Crystal structure of an activated Akt/protein kinase B ternary complex with GSK3-peptide and AMP-PNP. *Nat. Struct. Biol.* **2002**, *9*, 940–944.

(26) Skehan, P.; Storeng, R.; Scudiero, D.; Monks, A.; McMahon, J.; Vistica, D.; Warren, J. T.; Bokesch, H.; Kenney, S.; Boyd, M. R. New colorimetric cytotoxicity assay for anticancer-drug screening. *J. Natl. Cancer Inst.* **1990**, *82*, 1107–1112.

(27) Vlietstra, R. J.; van Alewijk, D. C.; Hermans, K. G.; van Steenbrugge, G. J.; Trapman, J. Frequent inactivation of PTEN in prostate cancer cell lines and xenografts. *Cancer Res.* **1998**, *58*, 2720–2723.

(28) Gowan, S. M.; Hardcastle, A.; Hallsworth, A. E.; Valenti, M. R.; Hunter, L.-J. K.; de Haven Brandon, A. K.; Garrett, M. D.; Raynaud, F.; Workman, P.; Aherne, W.; Eccles, S. A. Application of Meso Scale technology for the measurement of phospho-proteins in human tumour xenografts. *Assay Drug Dev. Technol.* **2007**, *5*, 391–401.

(29) Values of log P^{30} and TPSA were calculated using ChemDraw Ultra 10.0, CambridgeSoft.

(30) Ghose, A. K.; Crippen, G. M. Atomic physicochemical parameters for three-dimensional-structure-directed quantitative structure−activity relationships. 2. Modeling dispersive and hydrophobic interactions. *J. Chem. Inf. Comput. Sci.* **1987**, *27*, 21–35.

(31) Kinase selectivity was determined in SelectScreen, Invitrogen Ltd. Compounds were tested at 1 μM against the following enzymes: CDK2/cyclin2, CHK1, CHK2, CK2α1, EGFR, FGFR1, FLT3, GSK3β, IGFR1, JAK3, KDR, MAPK1, MAPKAPK2, PKCα, PKCδ, PKCγ, ROCK2, RSK2, p70S6K, SGK1, SRC.

(32) Bossis, I.; Stratakis, C. A. Minireview: PRKAR1A: normal and abnormal functions. *Endocrinology* **2004**, *145*, 5452–5458.

(33) Bossis, I.; Voutetakis, A.; Bei, T.; Sandrini, F.; Griffin, K. J.; Stratakis, C. A. Protein kinase A and its role in human neoplasia: the Carney complex paradigm. *Endocr. Relat. Cancer* **2004**, *11*, 265–280.

(34) Zhao, Z.; Leister, W. H.; Robinson, R. G.; Barnett, S. F.; Defeo-Jones, D.; Jones, R. E.; Hartman, G. D.; Huff, J. R.; Huber, H. E.; Duggan, M. E.; Lindsley, C. W. Discovery of 2,3,5-trisubstituted pyridine derivatives as potent Akt1 and Akt2 dual inhibitors. *Bioorg. Med. Chem. Lett.* **2005**, *15*, 905–909.

(35) Lindsley, C. W.; Zhao, Z.; Leister, W. H.; Robinson, R. G.; Barnett, S. F.; Defeo-Jones, D.; Jones, R. E.; Hartman, G. D.; Huff, J. R.; Huber, H. E.; Duggan, M. E. Allosteric Akt (PKB) inhibitors: discovery and SAR of isozyme selective inhibitors. *Bioorg. Med. Chem. Lett.* **2005**, *15*, 761–764.

(36) Harrington, L. S.; Findlay, G. M.; Gray, A.; Tolkacheva, T.; Wigfield, S.; Rebholz, H.; Barnett, J.; Leslie, N. R.; Cheng, S.; Shepherd, P. R.; Gout, I.; Downes, C. P.; Lamb, R. F. The TSC1-2 tumor suppressor controls insulin-PI3K signaling via regulation of IRS proteins. *J. Cell Biol.* **2004**, *166*, 213–223.

(37) Han, E. K.; Leverson, J. D.; McGonigal, T.; Shah, O. J.; Woods, K. W.; Hunter, T.; Giranda, V. L.; Luo, Y. Akt inhibitor A-443654 induces rapid Akt Ser-473 phosphorylation independent of mTORC1 inhibition. *Oncogene* **2007**, *26*, 5655–5661.

(38) Application of the Cheng−Prussof equation ($IC_{50} = K_i(1 + [ATP]/K_{m,ATP})$ to the PKBβ biochemical assay used in this work (PKBβ $K_{m,ATP} = 30$ μM, [ATP] = 30 μM). Experimental determination by variation of [ATP] of the K_i for other PKBβ inhibitors[21] has confirmed that $IC_{50} \approx 2K_i$ for this assay.

(39) Knight, Z. A.; Shokat, K. M. Features of selective kinase inhibitors. *Chem. Biol.* **2005**, *12*, 621–637.

(40) Smith, N. F.; Hayes, A.; James, K.; Nutley, B. P.; McDonald, E.; Henley, A.; Dymock, B.; Drysdale, M. J.; Raynaud, F. I.; Workman, P. Preclinical pharmacokinetics and metabolism of a novel diaryl pyrazole resorcinol series of heat shock protein 90 inhibitors. *Mol. Cancer Ther.* **2006**, *5*, 1628–1637.

(41) Moreno-Farre, J.; Workman, P.; Raynaud, F. I. Analysis of potential drug−drug interactions for anticancer agents in human liver microsomes by high throughput liquid chromatography/mass spectrometry assay. *Recent Adv. Res. Updates* **2006**, *7*, 207–224.

(42) Robins, R. K. Potential purine antagonists. I. Synthesis of some 4,6-substituted pyrazolo[3,4-*d*]pyrimidines. *J. Am. Chem. Soc.* **1956**, *78*, 784–790.

(43) Girgis, N. S.; Larson, S. B.; Robins, R. K.; Cottam, H. B. The synthesis of 5-azaindoles by substitution-rearrangement of 7-azaindoles upon treatment with certain primary amines. *J. Heterocycl. Chem.* **1989**, *26*, 317–325.

(44) Caldwell, J. J.; Cheung, K.-M.; Collins, I. Synthesis of 4-(cyclic dialkylamino)-7-azaindoles by microwave heating of 4-halo-7-azaindoles and cyclic secondary amines. *Tetrahedron Lett.* **2007**, *48*, 1527–1529.

(45) Xie, J.-S.; Huang, C. Q.; Fang, Y.-Y.; Zhu, Y.-F. A convenient synthesis of 1′-H-spiro-(indoline-3,4′-piperidine) and its derivatives. *Tetrahedron* **2004**, *60*, 4875–4878.

(46) Hulshof, J. W.; Vischer, H. F.; Verheij, M. H. P.; Fratantoni, S. A.; Smit, M. J.; de Esch, I. J. P.; Leurs, R. Synthesis and pharmacological characterization of novel inverse agonists acting on the viral-encoded chemokine receptor US28. *Bioorg. Med. Chem.* **2006**, *14*, 7213–7230.

(47) Caldwell, J. J.; Collins, I. Rapid synthesis of 4-benzyl-4-aminopiperidines by addition of Grignard reagents to *N*-(1-Boc-piperidin-4-ylidene)-*tert*-butanesulfinyl imine. *Synlett* **2006**, 2565–2568.

(48) Davoll, J. 26. Pyrrolo[2,3-*d*]pyrimidines. *J. Chem. Soc.* **1960**, 131–138.

(49) Sugiyama, M.; Sakamoto, T.; Kamigaki, Y.; Fukumi, H.; Itoh, K.; Satoh, Y.; Yamaguchi, T. Piperidineacrylate derivatives as potential antiallergy agents. *Chem. Pharm. Bull.* **1993**, *41*, 882–888.

JM701437D